JOC Article

# Enecarbamates as Selective Substrates in Oxidations: Chiral-Auxiliary-Controlled Mode Selectivity and Diastereoselectivity in the [2+2] Cycloaddition and Ene Reaction of Singlet Oxygen and in the Epoxidation by DMD and *m*CPBA

Waldemar Adam,*,† Sara G. Bosio,† Nicholas J. Turro,‡ and Barbara T. Wolff†

*Institut für Organische Chemie, Universität Würzburg, Am Hubland, D-97074 Würzburg, Germany, and Department of Chemistry, Columbia University, 3000 Broadway, New York, New York 10027*

*wadam@chemie.uni-wuerzburg.de*

*Received November 27, 2003*

The stereochemical course of the oxidation of chiral oxazolidinone-substituted enecarbamates has been studied for singlet oxygen ($^1O_2$), dimethyldioxirane (DMD), and *m*-chloroperbenzoic acid (*m*CPBA) by examining of the special structural and stereoelectronic features of the enecarbamates. Valuable mechanistic insight into these selective oxidations is gained. Whereas the $R^1$ substituent on the chiral auxiliary is responsible for the steric shielding of the double bond and determines the sense of the $\pi$-facial diastereoselectivity, structural characteristic such as the *Z*/*E* configuration and the nature of the $R^2$ group on the double bond are responsible for the extent of the diastereoselectivity. Stereoelectronic steering by the vinylic nitrogen functionality controls the mode selectivity (ene reaction vs [2+2] cycloaddition) in the case of $^1O_2$.

## Introduction

Chiral auxiliaries have been successfully employed in controlling the diastereoselectivity of numerous oxygen-transfer reactions[1] such as photooxygenations[2] and epoxidations.[3] The control of the stereochemical course of these reactions is of general synthetic interest, because it gives access to enantiomerically pure oxygen-functionalized building blocks.[4]

The best results so far in auxiliary-controlled singlet oxygen reactions were obtained for substrates in which the chiral auxiliary (oxazolidine or oxazolidinone) was attached to a carbonyl functionality and not directly to the double bond. Through the appropriate choice of the chiral inductor, it is possible to control the diastereoselectivity of the [4+2] cycloaddition of $^1O_2$ with sorbic amide through steric interactions,[5] whereas the ene reaction with optically active oxazolidines, equipped with a urea functionality, have been steered through hydrogen bonding.[6] Most recently, we also showed that the diastereoselectivity of the [2+2] cycloaddition of singlet oxygen may be subject to control, when the oxazolidinone chiral auxiliary is directly attached to the reactive double bond in the form of an enecarbamate functionality.[4]

To date, the enecarbamates, readily prepared from the corresponding aldehyde and an optically active oxazolidinone auxiliary, have hardly[7] been used to direct the diastereoselectivity of reactions that involve their CC double bond. In view of their special structural and electronic features, these unusual substrates offer promising opportunities to explore their propensity in stereoselective oxidations. Variation of their structural features, namely, the *R*/*S* configuration of the stereogenic center, the size of the $R^1$ substituent of the oxazolidinone auxiliary, and the *E*/*Z* geometry of the CC double bond, as well as the type of $R^2$ substituent, enables a high measure of steric manipulation in directing the attacking oxidant.

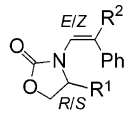


$R^1$= H, Me, $^i$Pr, Ph, $^t$Bu
$R^2$= Me, $CH(CH_3)_2$, $CH(CH_3)Ph$

Moreover, a definite advantage for stereochemical control through such steric effects derives from the fact that in these enecarbamates the distance between the stereogenic center of the chiral auxiliary and the reactive

† Universität Würzburg.
‡ Columbia University.

(1) Jones, S. J. *Chem. Soc., Perkin Trans. 1* **2002**, *95*, 1−21. Bonini, C.; Righi, G. *Tetrahedron* **2002**, *58*, 4981−5184.

(2) (a) Adam, W.; Griesbeck, A. *Synthesis* **1986**, 1050−1052. (b) Dussault, P. H.; Woller, K. R.; Hillier, M. C. *Tetrahedron* **1994**, *50*, 8929−8940. (c) Adam, W.; Wirth, T.; Pastor, A.; Peters, K. *Eur. J. Org. Chem.* **1939**, *4*, 501−506. (d) Adam, W.; Güthlein, M.; Peters, E.-M.; Peters, K.; Wirth, T. *J. Am. Chem. Soc.* **1998**, *120*, 4091−4093. (e) Adam, W.; Degen, H.-G.; Krebs, O.; Saha-Moller, C. R. *J. Am. Chem. Soc.* **2002**, *124*, 12938−12939. (f) Adam, W.; Bosio, S. G.; Turro, N. J. *J. Am. Chem. Soc.* **2002**, *124*, 8814−8815; (g) Adam, W.; Bosio, S. G.; Turro, N. J. *J. Am. Chem. Soc.* **2002**, *124*, 14004−14005;

(3) (a) Adam, W.; Pastor, A.; Peters, K.; Peters, E.-M. *Org. Lett.* **2000**, *2*, 1019−1022. (b) Adam, W.; Schambony, S. B. *Org. Lett.* **2001**, *3*, 79−82. (c) Adam, W.; Bosio, S. G.; Wolff, B. T. *Org. Lett.* **2003**, 819−822.

(4) Adam, W.; Bosio, S. G.; Turro, N. J. *J. Am. Chem. Soc.* **2002**, *124*, 8814−8815.

(5) Adam, W.; Güthlein, M.; Peters, E.-M.; Peters, K.; Wirth, T. *J. Am. Chem. Soc.* **1998**, *120*, 4091−4093.

(6) Adam, W.; Peters, K.; Peters, E.-M.; Schambony, S. B. *J. Am. Chem. Soc.* **2000**, *122*, 7610−7611.

10.1021/jo035745c CCC: $27.50 
Published on Web 02/06/2004

**TABLE 1. Synthesis of the Diastereomeric Enecarbamates 1**

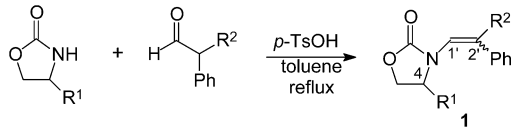


| entry | enecarbamate | $R^1$ | $R^2$ | dr[a] *Z*:*E* |
|---|---|---|---|---|
| 1 | **1a** | H | Ph(Me)CH | >95:5 |
| 2 | (4*R*)-**1b** | *R*-Me | Ph(Me)CH | >95:5 |
| 3 | (4*R*)-**1c** | *R*-$^i$Pr | Ph(Me)CH | >95:5 |
| 4 | (4*S*)-**1d** | *S*-$^i$Pr | Ph(Me)CH | >95:5 |
| 5 | (4*S*)-**1e** | *S*-Ph | Ph(Me)CH | >95:5 |
| 6 | (4*S*)-**1f** | *S*-$^t$Bu | Ph(Me)CH | >95:5 |
| 7 | (4*R*)-**1g** | *R*-$^i$Pr | $^i$Pr | >95:5 |
| 8 | **1h** | H | Me | 53:47 |
| 9 | (4*R*)-**1i** | *R*-Me | Me | 73:27 |
| 10 | (4*R*)-**1j** | *R*-$^i$Pr | Me | 71:29 |
| 11 | (4*S*)-**1k** | *S*-Ph | Me | 50:50 |
| 12 | (4*S*)-**1*l*** | *S*-$^t$Bu | Me | 83:17 |

[a] Yields >95% in all cases; the diastereomeric ratios were determined from the areas under the characteristic signals in the $^1$H NMR spectra directly on the crude reaction mixture (error ±5% of the stated value); for ratios >95:5, the minor diastereomer was not detected; material balances >95%.

CC double bond functionality is significantly less compared to the usual Evans' oxazolidinone auxiliary,[8] linked by means of an amide functionality.[9]

As oxidants we have chosen singlet oxygen, dimethyldioxirane, and *m*-chloroperbenzoic acid to examine the stereoselectivity of the photooxygenation and epoxidation as a function of the size and type of $R^1$ and $R^2$ substituents and the *E*/*Z* geometry of the enamine-type double bond. For the photooxygenation it was also of mechanistic interest to assess the competition between [2+2] cycloaddition and the ene reaction, when the $R^2$ substituent carries allylic hydrogen atoms. Analogous to the stereoelectronic directing effect observed in vinyl ethers,[10] it was expected that such mode selectivity should also be expressed by the enamine-type functionality, dependent on its *E*/*Z* configuration.

Herein we present the results of our extensive study, which provides valuable mechanistic insight into the selective oxidations by singlet oxygen, DMD, and *m*CPBA, as well as promising applications.

## Results

**Synthesis and Configurational Assignment of the Enecarbamates 1.** The enecarbamates **1** (Table 1) were obtained in high yield (>95%) by refluxing the chiral oxazolidinones[9] and the various aldehydes in toluene, catalyzed by *p*-toluenesulfonic acid. In the case of enecarbamates **1a**−**f**, the only double bond diastereomer obtained from the condensation of 2,3-diphenylbutanal with the corresponding oxazolidinone was the *Z* one (Table 1, entries 1−6), as was proved by NOESY measurements (see the Supporting Information). A high selectivity was also observed when 2,3-diphenylbutanal was replaced by 3-methyl-2-phenylbutanal (**1g**, entry 7).

By condensing the different oxazolidinones with the 2-phenylpropanal, the enecarbamates **1h**−***l*** were obtained (entries 8−12). In these cases both double bond

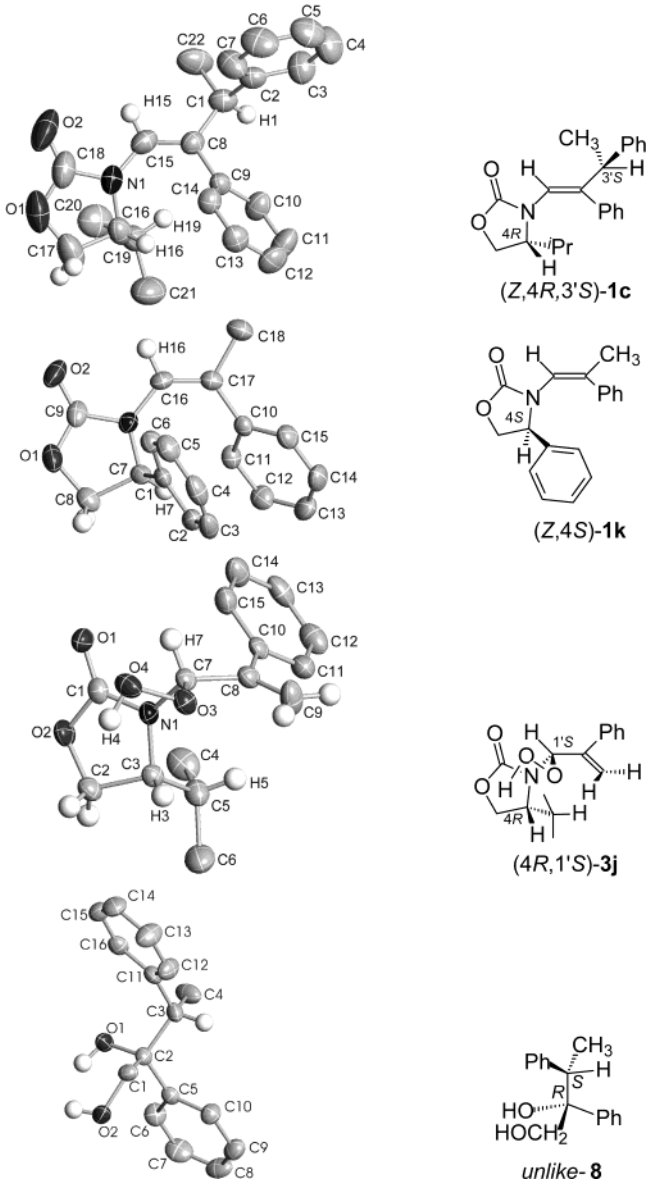


**FIGURE 1.** Crystal structures of the enecarbamates (*Z*,4*R*,3′*S*)-**1c** (ref 2f) and (*Z*,4*S*)-**1k** (see the Supporting Information), the hydroperoxide (4*R*,1′*S*)-**3j** (ref 2g), and the diol *unlike*-**8** (ref 2f).

(7) Janey, J. M.; Iwama, T.; Kozmin, S. A.; Rawal, V. H. *J. Org. Chem.* **2000**, *65*, 9059−9068. Xiong, H.; Hsung, R. P.; Shen, L.; Hahn J. M. *Tetrahedron Lett.* **2002**, 4449−4453. Xiong, H.; Hsung, R. P.; Berry, C. R.; Rameshkumar, C. *J. Am. Chem. Soc.* **2001**, *123*, 7174−7175. Rameshkumar, C.; Xiong, H.; Tracey, M. R.; Berry, C. R.; Yao, L. J.; Hsung, R. P. *J. Org. Chem.* **2002**, *67*, 1339−1345.

(8) (a) Evans, D. A.; Chapman, K. T.; Bisaha, J. *J. Am. Chem. Soc.* **1988**, *110*, 1238−1256. (b) Evans, D. A.; Urpi, F.; Somers, T. C.; Clark, J. S.; Bilodeau, M. T. *J. Am. Chem. Soc.* **1990**, *112*, 8215−8216. (c) Evans, D. A.; Nelson, S. G. *J. Am. Chem. Soc.* **1988**, *110*, 1238−1256. (d) Ager, D. J.; Prakash I.; Schaad, D. R. *Aldrichim. Acta* **1997**, *30*, 3−12.

(9) (a) Evans, D. A.; Chapman, K. T.; Bisaha, J. *J. Am. Chem. Soc.* **1988**, *110*, 1238−1256. (b) Evans, D. A.; Urpi, F.; Somers, T. C.; Clark, J. S.; Bilodeau, M. T. *J. Am. Chem. Soc.* **1990**, *112*, 8215−8216. (c) Evans, D. A.; Nelson, S. G. *J. Am. Chem. Soc.* **1997**, *119*, 9309−9310. (d) Ager, D. J.; Prakash I.; Schaad, D. R. *Aldrichim. Acta* **1997**, *30*, 3−12.

(10) (a) Rousseau, G.; Le Perchec, P.; Conia, J. M. *Tetrahedron Lett.* **1977**, 2517−2520. (b) Lerdal, D.; Foote, C. S. *Tetrahedron Lett.* **1978**, 3227−3230. (c) Inagaki, S.; Fujimoto, H.; Fukui, K. *Chem. Lett.* **1976**, 749−752.

**TABLE 2. Mode and Diastereochemical Selectivities in the Photooxygenation of the Enecarbamates 1[a]**

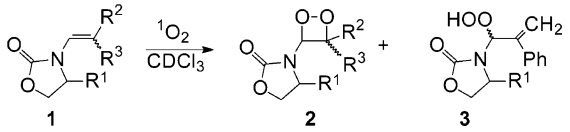


| | | | | | selectivity[b] | | |
|---|---|---|---|---|---|---|---|
| | | | | | mode | diastereo | |
| entry | substrate | $R^1$ | $R^2$ | $R^3$ | [2+2]:ene **2**:**3**[c] | ene *ul*:*lk* | [2+2] (1*S*,2*S*):(1*R*,2*R*) |
| 1 | **1a** | H | Ph(Me)CH | Ph | >95 | | 50:50 |
| 2 | (*Z*,4*R*,3′*S*)-**1b** | *R*-Me | (*S*)-Ph(Me)CH | Ph | >95 | | >95:5 |
| 3 | (*Z*,4*R*,3′*R*)-**1b** | *R*-Me | (*R*)-Ph(Me)CH | Ph | >95 | | >95:5 |
| 4 | (*Z*,4*R*,3′*R*)-**1c** | *R*-$^i$Pr | (*R*)-Ph(Me)CH | Ph | >95 | | >95:5 |
| 5 | (*Z*,4*R*,3′*S*)-**1c** | *R*-$^i$Pr | (*S*)-Ph(Me)CH | Ph | >95 | | >95:5 |
| 6 | (*Z*,4*S*,3′*S*)-**1d** | *S*-$^i$Pr | (*S*)-Ph(Me)CH | Ph | >95 | | <5:95 |
| 7[d] | (*Z*,4*R*,3′*R*)-**1c** | *R*-$^i$Pr | (*R*)-Ph(Me)CH | Ph | >95 | | >95:5 |
| 8[e] | (*Z*,4*R*,3′*R*)-**1c** | *R*-$^i$Pr | (*R*)-Ph(Me)CH | Ph | >95 | | >95:5 |
| 9 | (*Z*,4*S*,3′*R*)-**1e** | *S*-Ph | (*R*)-Ph(Me)CH | Ph | >95 | | <5:95 |
| 10 | (*Z*,4*S*,3′*S*)-**1e** | *S*-Ph | (*S*)-Ph(Me)CH | Ph | >95 | | <5:95 |
| 11 | (*Z*,4*S*,3′*R*)-**1f** | *S*-$^t$Bu | (*R*)-Ph(Me)CH | Ph | >95 | | <5:95 |
| 12 | (*Z*,4*S*,3′*S*)-**1f** | *S*-$^t$Bu | (*S*)-Ph(Me)CH | Ph | >95 | | <5:95 |
| 13 | (*Z*,4*R*)-**1g** | *R*-$^i$Pr | $^i$Pr | Ph | >95 | | >95:5 |
| 14 | *E*-**1h** | H | Ph | Me | 15:85 | | |
| 15 | *Z*-**1h** | H | Me | Ph | 80:20 | | |
| 16 | (*E*,4*R*)-**1i** | *R*-Me | Ph | Me | 16:84 | 88:12 | n.d. |
| 17 | (*E*,4*R*)-**1j** | *R*-$^i$Pr | Ph | Me | 36:64 | 83:17 | n.d. |
| 18 | (*E*,4*S*)-**1k** | *S*-Ph | Ph | Me | 8:92 | 71:29 | n.d. |
| 19 | (*E*,4*S*)-**1*l*** | *S*-$^t$Bu | Ph | Me | 23:77 | 91:9 | n.d. |
| 20 | (*Z*,4*R*)-**1i** | *R*-Me | Me | Ph | 80:20 | 53:47 | >95:5 |
| 21 | (*Z*,4*R*)-**1j** | *R*-$^i$Pr | Me | Ph | 75:25 | 56:44 | >95:5 |
| 22 | (*Z*,4*S*)-**1k** | *S*-Ph | Me | Ph | 87:13 | 85:15 | <5:95 |
| 23 | (*Z*,4*S*)-**1*l*** | *S*-$^t$Bu | Me | Ph | 60:19[f] | >95:5 | <5:95 |

[a] The photooxygenations were run in $CDCl_3$ at −32 °C with TPFPP (5,10,15,20-tetrakis(pentafluorophenyl)porphine) as sensitizer until complete conversion of the enecarbamate. [b] Determined from the areas under the characteristic signals in the $^1$H NMR spectrum directly on the photooxygenate (error ±5% of the stated value); material balance >95% for all reactions. [c] In entries 1−13, the ene product corresponding to **3** was not observed. [d] $CD_3OD$:$CDCl_3$ (4.1:1). [e] $CD_3COCD_3$:$CDCl_3$ (2.4:1). [f] Also 21% of the endoperoxide **6*l*** was obtained.

isomers were formed, and the *E*/*Z* ratio depended on the individual substituent in the oxazolidinone ring. After chromatographic separation of the *E*/*Z* isomers on silica gel, the double bond configuration was proved by NOESY measurement; in the case of (*Z*,4*S*)-**1k**, an X-ray analysis of one of the diastereomers confirmed the proposed structure (Figure 1).

The unsubstituted enecarbamate **1h** and the phenyl derivative **1k** were formed nondiastereoselectively (ca. 50:50 mixture of the two double bond isomers), whereas the methyl and the isopropyl substituents gave appreciable amounts of the *E* diastereomers. The *tert*-butyl-substitueted enecarbamate (4*S*)-**1*l*** displayed the highest *E* selectivity; evidently, the steric repulsion of the demanding *tert*-butyl substituent with the phenyl group on the double bond is the most effective.

**Photooxygenations.** The photooxygenation of the enecarbamates **1** was performed at −35 °C with 5,10,15,20-tetrakis(pentafluorophenyl)porphine (TPFPP) as the sensitizer and a 800-W sodium lamp as the light source. In the enecarbamates **1a**−**f**, the 1-phenylethyl substituent at the C2′ position of the double bond was chosen to minimize the ene reaction, since the required coplanar alignment of the only allylic hydrogen atom[11] is conformationally encumbered. Indeed, for these enecarbamates, only [2+2] cycloaddition was observed. The dioxetanes **2** could not be isolated, because they readily decomposed at room temperature (ca. 20 °C) to the expected carbonyl products, especially on attempted silica gel chromatography.

The photooxygenation of the unsubstituted enecarbamate **1a** displayed no diastereoselectivity (Table 2, entry 1), whereas already the methyl derivative (*Z*,4*R*)-**1b** (Table 2, entries 2 and 3), and certainly the isopropyl derivative (*Z*,4*R*)-**1c** (entries 4 and 5), afforded the diastereomerically pure dioxetanes (4*R*,3′*S*,4′*S*)-**2b** and (4*R*,3′*S*,4′*S*)-**2c**. The other possible diastereomers could not be observed even in the 600-MHz $^1$H NMR spectra of the photooxygenate.

The change of the configuration for the $R^1$ substituent in the oxazolidinone from *R* to *S* has as a consequence the inversion of the configuration at the newly formed stereogenic centers in the dioxetane **2c**, i.e., 4*R*,3′*S*,4′*S* versus 4*S*,3′*R*,4′*R* (entries 5 and 6). Also in the polar solvent mixtures $CD_3OD$:$CDCl_3$ (4.1:1, entry 7) and $CD_3COCD_3$:$CDCl_3$ (2.4:1, entry 8), the diastereomerically pure dioxetane (4*R*,3′*S*,4′*S*,1″*R*)-**2c** was formed in the photooxygenation of enecarbamate (*Z*,4*R*,3′*R*)-**1c**.

The photooxygenation of (*Z*,4*S*,3′*R*)-**1e** and (*Z*,4*S*,3′*S*)-**1e** ($R^1$ = Ph, entries 9 and 10) and (*Z*,4*S*,3′*R*)-**1f** and (*Z*,4*S*,3′*S*)-**1f** ($R^1$ = $^t$Bu, entries 11 and 12) showed also a diastereoselectivity of >95:5 in the formation of the dioxetanes (4*S*,3′*R*,4′*R*)-**2e** and (4*S*,3′*R*,4′*R*)-**2f**. The photooxygenation of enecarbamate (*Z*,4*R*)-**1g**, in which the

(11) Gollnick, K.; Hartmann, H.; Paur, H. In *Oxygen and Oxy-Radicals in Chemistry and Biology*; Rodgers, M. A. J., Powers, E. L., Eds.; Academic Press: New York, 1981; pp 379−395.

**TABLE 3. Diastereoselectivities of the Epoxidation of Enecarbamates 1 by DMD and *m*CPBA**

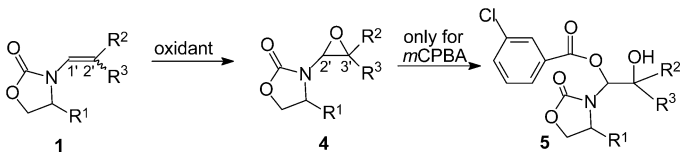


| entry | substrate | reagent | $R^1$ | $R^2$ | $R^3$ | diastereoselectivity[a] 2′*S*:2′*R* |
|---|---|---|---|---|---|---|
| 1 | *Z*-**1h** | DMD | H | Ph | Me | 50:50 |
| 2 | *Z*-**1h** | *m*CPBA | H | Ph | Me | 50:50 |
| 3a | (*Z*,4*R*)-**1j** | DMD | *R*-$^i$Pr | Ph | Me | 60:40 |
| 3b | (*Z*,4*R*)-**1j** | DMD | *R*-$^i$Pr | Ph | Me | 63:37 |
| 4 | (*Z*,4*R*)-**1j** | *m*CPBA | *R*-$^i$Pr | Ph | Me | 70:30 |
| 5 | (*Z*,4*S*)-**1k** | DMD | *S*-Ph | Ph | Me | 8 (10):92 (90) |
| 6 | (*Z*,4*S*)-**1k** | *m*CPBA | *S*-Ph | Ph | Me | 8 (7):92 (93) |
| 7 | (*Z*,4*S*)-**1*l*** | DMD | *S*-$^t$Bu | Ph | Me | 7 (6):93 (94) |
| 8 | (*Z*,4*S*)-**1*l*** | *m*CPBA | *S*-$^t$Bu | Ph | Me | 7:93 |
| 9 | *E*-**1h** | DMD | H | Me | Ph | 50:50 |
| 10 | *E*-**1h** | *m*CPBA | H | Me | Ph | 50:50 |
| 11 | (*E*,4*R*)-**1j** | DMD | *R*-$^i$Pr | Me | Ph | 53:47 |
| 12 | (*E*,4*R*)-**1j** | *m*CPBA | *R*-$^i$Pr | Me | Ph | 50:50 |
| 13 | (*E*,4*S*)-**1k** | DMD | *S*-Ph | Me | Ph | 40:60 |
| 14 | (*E*,4*S*)-**1k** | *m*CPBA | *S*-Ph | Me | Ph | 48:52[b] |
| 15 | (*E*,4*S*)-**1*l*** | DMD | *S*-$^t$Bu | Me | Ph | 25 (25):75 (75) |
| 16 | (*E*,4*S*)-**1*l*** | *m*CPBA | *S*-$^t$Bu | Me | Ph | 21:79 |
| 17 | **1a** | DMD | H | *rac*-Ph(Me)CH | Ph | <5:95 |
| 18 | (*Z*,4*R*,3′*R*)-**1c** | DMD | *R*-$^i$Pr | (*R*)-Ph(Me)CH | Ph | <5:95 |
| 19 | (*Z*,4*R*,3′*S*)-**1c** | DMD | *R*-$^i$Pr | (*S*)-Ph(Me)CH | Ph | 34:66 |

[a] Diastereoselectivities were determined by $^1$H NMR spectroscopy (error ±5% of the stated value) directly on the reaction mixture and by HPLC analysis (error ±2% of the stated value); the results of the diol **10** prepared from epoxide **4** (DMD reactions) and from the ester **5** (*m*CPBA reactions) are given in parentheses. [b] Also 50% epoxide (2′*S*,3′*R*)-**4d** and 2% ester (2′*S*,3′*R*)-**5d** were obtained. In Table 3, only the configurations at the C2′ position are given, namely the stereochemical descriptors 2′*S* and 2′*R*, because this position does not depend on the initial double bond configuration of the enecarbamates *Z*-1 and *E*-1. For clarity and convenience, the 2′*S* and 2′*R* descriptors are marked in bold face in the text.

phenylethyl substituent on the double bond is replaced by an isopropyl substituent, gave exclusively the dioxetane (4*R*,3′*S*,4′*S*)-**2g** (entry 13).

The enecarbamates **1h**−***l*** all possess ene-active allylic hydrogen and, thus, the [2+2] cycloaddition is competed for by the ene reaction. The *Z*- and *E*-configured enecarbamates displayed a substantial difference in the mode selectivity: Whereas the photooxygenation of the enecarbamates *E*-**1** proceeded preferably along the ene mode to the hydroperoxides **3** (entries 14 and 16−19), the *Z*-**1** diastereomers yielded mainly the [2+2]-cycloadducts **2** (entries 15 and 20−23).

The diastereoselectivity of the ene reaction with the ene carbamates ***E*-1** ranges from 71:29 for enecarbamate (*E*,4*S*)-**1k** (entry 18) to 91:9 for (*E*,4*S*)-**1*l*** (entry 19); no diastereomers are possible for the enecarbamate ***E*-1h** ($R^1$ = H, entry 14). In contrast, the ene reaction of the *Z*-**1** isomers covered a wide spread in the diastereomeric ratios, which extended from essentially unselective for (*Z*,4*R*)-**1i** ($R^1$ = Me, entry 20) and (*Z*,4*R*)-**1j** ($R^1$ = $^i$Pr, entry 21) to highly selective for (*Z*,4*S*)-**1k** ($R^1$ = Ph, entry 22) and expectedly (*Z*,4*S*)-**1*l*** ($R^1$ = $^t$Bu, entry 23). For both sets of ene products, the major diastereomer has the *unlike* configuration and the extent in the facial differentiation follows the steric demand of the $R^1$ substituent in the oxazolidinone ring. Furthermore, the diastereofacial differentiation is more pronounced for the *Z* (entries 20−23) than the *E* isomers (entries 16−19).

The diastereoselectivity of the [2+2] cycloaddition is essentially perfect in the case of the enecarbamates *Z*-**1** (entries 20−23), except for *Z*-**1h** ($R^1$= H, entry 15), which has no stereogenic centers and cannot display any diastereoselectivity. In the case of the enecarbamates *E*-**1**, the diastereoselectivity could not be determined, because the dioxetanes were too labile and only the decomposition products were detected and no conclusion could be reached on the diastereoselectivity of the *Z* versus *E* enecarbamates.

**Epoxidation with DMD and *m*CPBA.** The enecarbamates **1h** and **1j**−***l*** were epoxidized by dimethyldioxirane (DMD) in acetone and *m*-chloroperbenzoic acid (*m*CPBA) in chloroform (Table 3) within a few hours at 20 °C. The epoxidation of the achiral substrates *Z*-**1h** ($R^1$ = H, entry 1) and *E*-**1h** (entry 9) by DMD gave, as expected, a 50:50 mixture of the diastereomeric epoxides. The epoxidation of the chiral (*Z*,4*R*)-**1j** ($R^1$ = $^i$Pr) at 20 °C gave a mixture of the diastereomeric epoxides **4j** in a 2′*S*:2′*R* diastereomeric ratio (dr) of only 60:40 (entry 3a);[1] no significant increase in the dr value was observed at −25 °C (entry 3b).

An increase in the size of the substituent $R^1$ on the oxazolidinone ring caused a significant increase in the diastereoselectivity of the epoxidation by DMD: For the enecarbamate (*Z*,4*S*)-**1k** ($R^1$ = Ph, entry 5), the major epoxide isomer (**2′*R***,3′*R*)-**4k** was obtained in a high diastereomeric ratio (92:8); this was also the case with (*Z*,4*S*)-**1*l*** ($R^1$ = $^t$Bu, entry 7), for which the major diastereomer was (**2′*R***,3′*R*)-**4*l***. The epoxidation of the *E*-**1** isomers by DMD showed the same trend, in that for the achiral *E*-**1h** ($R^1$ = H) no selectivity was observed (entry 9), whereas the 2′*S*:2′*R* ratios range from 53:47 for (*E*,4*R*)-**1j** ($R^1$ = $^i$Pr, entry 11), to 40:60 for (*E*,4*S*)-**1k** ($R^1$ = Ph, entry 13), to 25:75 for (*E*,4*S*)-**1*l*** ($R^1$ = $^t$Bu, entry 15), that

**TABLE 4. Transformation of the Dioxetanes 2a,c,g,k to the Diols 8−10 for the Chemical Correlation of Their Configurations**

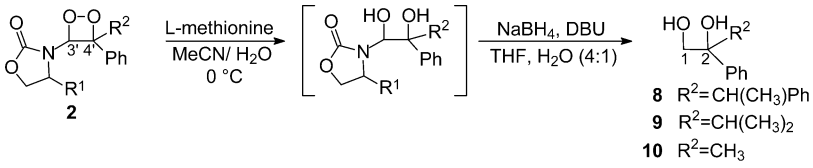


| entry | substrate | $R^1$ | $R^2$ | yield (%) | product | 2*S*:2*R*[a] |
|---|---|---|---|---|---|---|
| 1 | (4*R*,3′*S*,4′*S*,1″*R*)-**2c** | *R*-*i*Pr | (*R*)-Ph(Me)CH | 30 | *unlike*-**8** | >95:5 |
| 2 | (4*R*,3′*S*,4′*S*,1″*S*)-**2c** | *R*-*i*Pr | (*S*)-Ph(Me)CH | 35 | *like*-**8** | >95:5 |
| 3 | **2a** | H | *rac*-Ph(Me)CH | 25 | **8** | 50:50 |
| 4 | (4*R*,3′*S*,4′*S*)-**2g** | *R*-*i*Pr | $(CH_3)_2CH$ | 41 | **9** | >95:5 |
| 5 | (4*S*,3′*R*,4′*R*)-**2k** | *S*-Ph | $CH_3$ | 30 | **10** | <5:95 |

[a] Diastereoselectivity determined by HPLC analysis (2% error of the stated value) of the diols **8**−**10**; the HPLC analyses were carried out on chiral columns (Daicel CHIRALCEL OD-H) on a Kontron instrument, furnished with a UVIKON 720 spectrophotometer and a CHIRALYSER 1.6 from IBZ Massetechnik (Hannover, Germany).

is, the diastereoselectivity increases with the size of the $R^1$ substituent, but only moderately.

In the epoxidation with *m*CPBA, only a low conversion (ca. 10%) of the enecarbamates **1h** and **1j**−***l*** was observed directly in the $^1$H NMR spectrum of the reaction mixture. The major epoxide diastereomer was in all cases the same as that in the DMD reaction. Unfortunately, under these reaction conditions, the epoxide was opened exclusively at the C2′ position to the ester **5** by the acid generated from *m*CPBA, which could not be avoided by using aqueous $NaHCO_3$ as buffer (not shown in Table 3).

As expected, the achiral substrate *Z*-**1h** ($R^1$ = H, entry 2) was epoxidized unselectively by *m*CPBA. The diastereoselectivity in the epoxidation of the chiral enecarbamates *Z*-**1j**−***l*** increases as the size of the $R^1$ substituent on the oxazolidinone ring is increased. Thus, the dr values range from 70:30 (2′*S*:2′*R*) for the isopropyl-substituted enecarbamate (*Z*,4*R*)-**1j** (entry 4), to 8:92 for the phenyl-substituted derivative (*Z*,4*S*)-**1k** (entry 6), to 7:93 for the *tert*-butyl one (*Z*,4*S*)-***1l*** (entry 8). The *E*-configured enecarbamates (entries 12, 14, and 16) were epoxidized by *m*CPBA in a lower diastereoselectivity than the *Z*-configured counterparts (entries 4, 6, and 8), as was the case for DMD (entries 3, 5, and 7 versus 11, 13, and 15). Only for the substrate with the large *tert*-butyl substituent (*E*,4*S*)-***1l*** (entry 16) was an appreciable dr value of 21:79 observed in favor of the (**2′*S***,3′*S*)-***4l*** isomer. The *m*CPBA epoxidation of the (*E*,4*S*)-**1k** ($R^1$ = Ph) enecarbamate is unusual in that for this substrate the (**2′*R***,3′*S*)-**4k** diastereomer is ring-opened to the ester (**2′*S***,3′*S*)-**5k**, whereas the (**2′*S***,3′*R*)-**4k** epoxide persists esterification. Presumably, the nucleophilic attack of the *m*-chlorobenzoic acid on the C2′ position of the latter epoxide is sterically hindered.

To assess the influence of an additional stereogenic center within the enecarbamate structure and to uncover a possible *match*/*mismatch* effect, the racemic enecarbamate **1a** and the optically active derivatives (*Z*,4*R*,3′*R*)-**1c** and (*Z*,4*R*,3′*S*)-**1c** were epoxidized. Thus, the enecarbamate **1a** was converted in high diastereoselectivity (>95:5, entry 17) to the epoxide (2′*S**,3′*S**,1″*S**)-**4a**. In contrast, the epoxidation of the enecarbamate (*Z*,4*R*,3′*R*)-**1c** with DMD (Scheme 1) proceeded very slowly and gave after 3 d at ca. 20 °C the epoxide (2′*R*,3′*R*,1″*R*)-**4c** in high diastereoselectivity (>95:5, entry 18) and 88% yield. The corresponding 3′*S*-diastereomeric enecarbamate (*Z*,4*R*,3′*S*)-**1c** was also fully epoxidized after 3 d (entry 19); however, the epoxides (2′*R*,3′*R*,1″*S*)-**4c** and (2′*S*,3′*S*,1″*S*)-**4c** were formed in a diastereomeric ratio of only 67:33. Clearly, this low $\pi$-facial differentiation for the (*Z*,4*R*,3′*S*)-**1c** enecarbamate compared to the high one for the (*Z*,4*R*,3′*R*)-**1c** diastereomer discloses a pronounced substrate inherent *match*/*mismatch* situation.

**SCHEME 1. Epoxidation of the Diastereomeric (*Z*,4*R*,3′*R*)-1c and (*Z*,4*R*,3′*S*)-1c Enecarbamates with DMD**

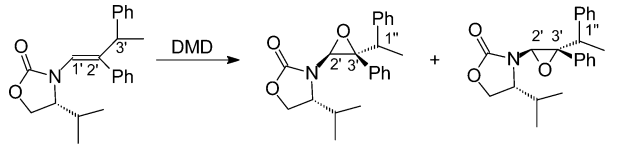


**SCHEME 2. Independent Synthesis of Authentic Diol *unlike*-8**

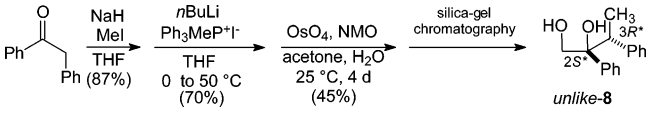


**Configurational Assignments.** The absolute configuration of the dioxetanes **2a**,**c**,**g**,**k** was established by reduction with L-methionine[12] (Table 4), followed by removal of the chiral auxiliary through treatment with $NaBH_4$/DBU[13] to afford the diols **8**−**10**. In the case of dioxetane (4*R*,3′*S*,4′*S*,1″*R*)-**2c** (entry 1), the *R* configuration at the C1″ position is known from an X-ray diffraction analysis of the *S*-configured enecarbamate diastereomer (*Z*,4*R*,3′*S*)-**1c** (Figure 1). The independent synthesis of diol **8** from desoxybenzoin (Scheme 2) gave a diastereomeric mixture (92:8) of the *unlike* and *like* products. The diastereomers were separated by silica gel chromatography and the NMR spectra of the *unlike* diastereomer [the relative configuration was determined by X-ray analysis (Figure 1)] were identical with those of the diol **8** obtained from the dioxetane (3′*S*,4′*S*,1″*R*)-

(12) Adam, W.; Hadjiarapoglou, L.; Mosandl, T.; Saha-Möller, C. R. *Angew. Chem., Int. Ed. Engl.* **1991**, *30*, 200−202.
(13) Gaul, C.; Schärer, K.; Seebach, D. *J. Org. Chem.* **2001**, *66*, 3059−3073.

**SCHEME 3. Assignment of the Absolute Configuration of the Dioxetane 2c by Chemical Correlation with Diol 8**

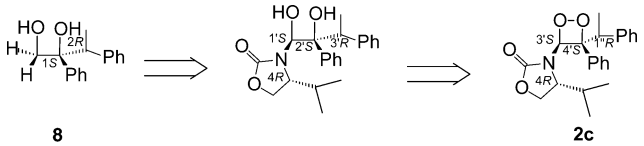

**SCHEME 4. Transformation of the Epoxide 4k and the Ester 5k to the Common Diol 10[a]**

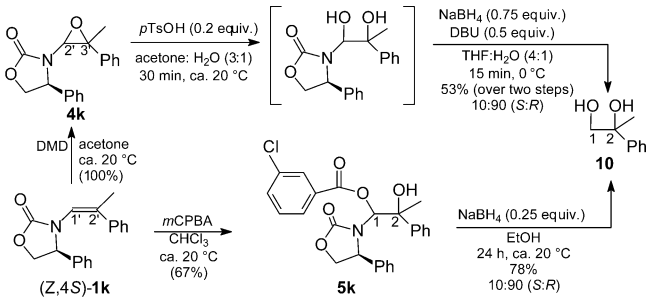

[a] The configuration refers to the major stereoisomer.

**2c**; hence, this diol is also *unlike* configured. In the 2,3-diphenyl-1,2-butanediol (**8**) derived from the dioxetane (3′*S*,4′*S*,1″*R*)-**2c**, the C2 stereogenic center (C1″ in the dioxetane) is already known to have the *R* configuration (Scheme 3), because the dioxetane was formed from the diastereomerically pure enecarbamate (*Z*,4*R*,3′*R*)-**1c**; thus, it follows that the C2 site in diol **8** possesses the *S* configuration, and the dioxetane **2c**, derived from (*Z*,4*R*,3′*R*)-**1c**, has the 4*R*,3′*S*,4′*S*,1″*R* configuration.

The absolute configuration of the dioxetane **2c**, obtained from (*Z*,4*R*,3′*S*)-**1c** (entry 2), was determined in the same way and the configuration was shown to be 4*R*,3′*S*,4′*S*,1″*S*. In the case of the dioxetane **2a** that pertains to enecarbamate **1a** (R′ = H), the transformation to the diol **8** gave a 50:50 diastereomeric mixture (entry 3).

By following the same procedure, the dioxetane (4*R*,3′*S*,4′*S*)-**2g** was derivatized to the known diol **9** (Table 4, entry 4) and characterized by chiral HPLC analysis. For this purpose, a racemic sample of the diol **9** (see the Supporting Information), whose HPLC data are known, was employed as reference.

The absolute configuration of the dioxetane (4*S*,3′*R*,4′*R*)-**2k** was determined by conversion to the corresponding diol **10** (Table 4, entry 5) and chiral HPLC analysis, with the enantiomerically pure diol as reference. The absolute configuration for the major diastereomer of the hydroperoxide **3j** was determined to be 4*R*,1′*S* (*unlike*) by means of X-ray analysis (Figure 1).

The absolute configurations of the epoxides **4** and esters **5** were assessed by their transformation to the common diol **10** (Scheme 4, shown exemplarily for the epoxide **4k** and the ester **5k**). The hydrolysis of the epoxide **4k** produced from the enecarbamate (*Z*,4*S*)-**1k** was catalyzed by *p*-toluenesulfonic acid (*p*-TsOH) in an acetone/water mixture, followed by reductive cleavage of the chiral auxiliary with $NaBH_4$/DBU. Similarly, the ester **5k** obtained in the *m*CPBA epoxidation of the enecarbamate (*Z*,4*S*)-**1k** was readily reduced to the diol **10** by $NaBH_4$. Chiral HPLC analysis of the resulting diol

**SCHEME 5. Assignment of the Relative Configuration of the Epoxide 4a by Chemical Correlation with Diol 8**

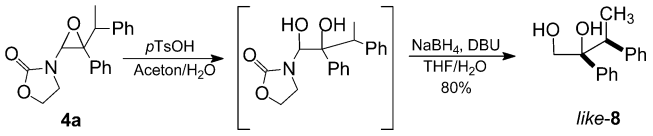

**10** gave the same enantiomeric ratio (10:90) as the diastereomeric ratios (8:92) of the epoxide **4k** and of the ester **5k** (within the experimental error). The absolute configuration of the major enantiomer was found to be *R* by comparison with an authentic reference sample of enantiomerically enriched diol **9**, prepared independently according to the literature[14] (see the Supporting Information).

With the configuration of the major enantiomer of diol **10** known to be *R*, the configuration at the C2 position in the major isomer of the epoxide **4k** and the ester **5k**, both derived from enecarbamate (*Z*,4*S*)-**1k**, may also be assigned *R*, provided that the C2 site is not involved in the ring-opening hydrolysis of **4k** and the esterification of **4k** to **5k**. That this is so could be unequivocally established for the latter process, since NMR analysis of the reaction mixture revealed that exclusively the regioisomer with nucleophilic attack on the C2′ position had been formed. Consequently, the absolute configuration of the ester **5k** is **1*S***,2*R* and, hence, that of the epoxide **4k** is **2′*R***,3′*R*.

The configurational assignment of the epoxides **4a** and **4c** derived from the DMD epoxidation of the enecarbamates **1a**, (*Z*,4*R*,3′*S*)-**1c**, and (*Z*,4*R*,3′*R*)-**1c** was achieved in analogy with that of epoxides **4j**,**k**. In the case of the diastereomerically pure racemic epoxide **4a**, hydrolysis afforded the *like* diastereomer of the diol **8** (Scheme 5). From the relative configuration of the diol *like*-**8**, the relative configuration of the epoxide **4a** was assigned to be (2′*S**,3′*S**,1″*S**)-**4a**.

According to the same procedure, the diastereomeric epoxide mixture of (2′*R*,3′*R*,1″*S*)-**4c** and (2′*S*,3′*S*,1″*S*)-**4c** was transformed to the diol **8**, whose *RS*:*SS*-diastereomeric ratio was determined to be 67:33 by chiral HPLC analysis. The same method was applied for the assignment of the diastereomerically pure epoxide **4c** derived from (*Z*,4*R*,3′*R*)-**1c**. The resulting diol *like*-**8** indicates the 2′*R*,3′*R*,1″*R* configuration for the newly formed stereogenic centers in the epoxide **4c**.

## Discussion

The results in Table 2 (photooxygenations) and Table 3 (epoxidations) show that the enecarbamates **1** are highly effective in controlling the diastereoselectivity of oxyfunctionalization by a number of electrophilic oxidants, which include singlet oxygen, DMD, and *m*CPBA. The characteristic structural features of the substrate, both of the oxazolidinone chiral auxiliary and of the CC double bond functionality, dictate the diastereoselective course of these oxidations through conformational effects. These derive mainly from steric interactions conditioned

(14) Sharpless, K. B.; Amberg, W.; Bennani, Y. L.; Crispino, G. A.; Hartung, J.; Joeng, K. S.; Kwong, H. L.; Morika, A. K.; Wang, Z. M.; Xu, D. Q.; Zhang, X. L. *J. Org. Chem.* **1992**, *57*, 2768−2771.

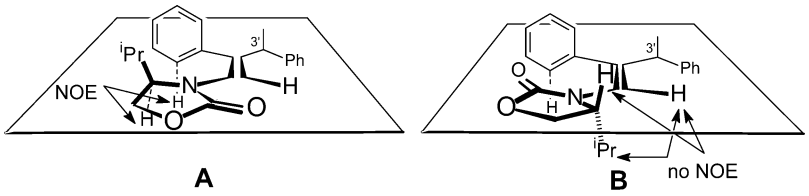


**FIGURE 2.** Possible conformations **A** and **B** of the enecarbamate (*Z*,4*R*)-**1c**.

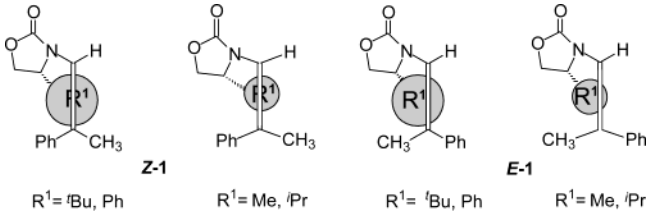


**FIGURE 3.** Distinct steric shielding for the enecarbamates *E*-**1** und *Z*-**1**.

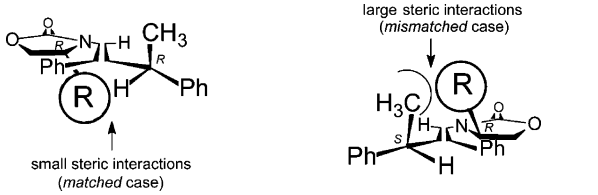


**FIGURE 4.** Steric interactions in the *matched* and *mismatched* cases of the enecarbamates **1**.

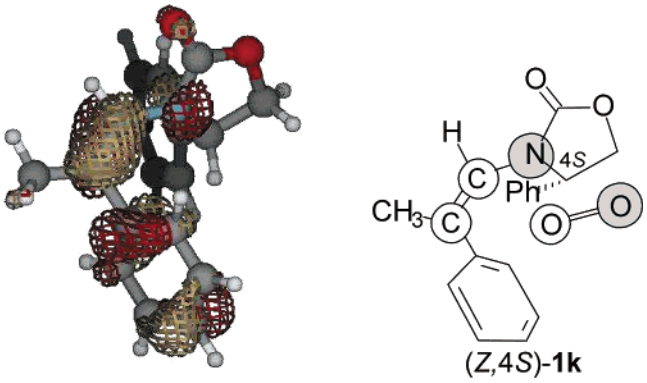


**FIGURE 5.** HOMO of the (*Z*,4*S*)-**1k** enecarbamate (calculated by the B3LYP method) and its orbital-directing effect of the singlet-oxygen attack.

on conformational effects, as well as from the stereoelectronic control in the attack of the oxidant (singlet oxygen). For convenience, we shall first enumerate these substrate-specific aspects and subsequently elaborate how they account for the observed selectivity.

**Structural and Stereoelectronic Characteristics of the Enecarbamates.** The preferred conformation of enecarbamate **1** plays an important role in the diastereochemical differentiation observed in this work. The shielding of only one side of the CC double bond is caused by the relative position of the chiral oxazolidinone with respect to the olefinic functionality. The X-ray structure of the enecarbamate (*Z*,4*R*,3′*S*)-**1c** (Figure 1) shows that a relatively small dihedral angle (ca. 38°) is favored between the carbonyl functionality and the CC double bond. For this reason, the $R^1$ substituent of the oxazolidinone occupies preferentially one of the half-spaces of the double bond and is thereby in an ideal position to interact sterically with the incoming oxidant. Of the two possible conformations **A** and **B** for the *Z*-configured enecarbamate **1c**, NOESY measurements reveal that in solution the conformer **A** dominates, in which the $R^1$ substituent and not the carbonyl group is directed toward the phenyl group at the double bond to minimize steric repulsions within the substrate molecule (Figure 2).

A relevant structural feature for stereochemical control is the distinct conformations of the double bond isomers *E*-**1** and *Z*-**1**. From DFT calculations (see the Supporting Information) it is apparent that the $R^1$ substituent ($^t$Bu, Ph) covers up the CC double bond better in the *Z* isomers than in the *E* case (Figure 3), which results in more effective shielding of the CC double bond; thus, a higher stereochemical control is expected for the *Z*-configured than for the *E*-configured enecarbamates. For the *Z* isomer, already the sterically less demanding methyl and isopropyl substituents promote a better diastereodifferentiation than for the corresponding *E* isomer (Figure 3).

An interesting structural feature offers the presence of an additional stereogenic carbon atom in the olefinic functionality of the enecarbamates **1**: The stereochemical course of the reaction may be influenced through the "*match*−*mismatch*" effect for the two possible diastereomers (Figure 4). As the structures reveal, the steric interactions between the two stereocenters in the *R*,*R* diastereomer are less severe compared with those in the *R*,*S* diastereomer, such that distinct conformations are expected and, consequently, differences in the stereochemical control occur.

An important stereoelectronic feature of the enecarbamates stems from the presence of the vinylic nitrogen functionality. In the photooxygenation of the enecarbamates **1**, this lone-pair-bearing substituent plays the same role that is taken by the methoxy group in the photooxygenation of methoxy styrenes.[10] Analogous to this well-documented "methoxy effect",[15] which depends on the stereoelectronic interaction between the lone pair of the methoxy group and the incoming singlet oxygen, also in the case of the enecarbamates **1**, the lone pair of the vinylic nitrogen steers the attack of the singlet oxygen preferentially to the side of the double bond that bears the oxazolidinone chiral auxiliary (Figure 5).

On the basis of these structural and stereoelectronic characteristics of the enecarbamates **1**, we shall now rationalize the selectivities observed in the oxidation of these mechanistically informative substrates. First we shall discuss separately the mechanistic aspects of the photooxygenation and epoxidation and subsequently point out conclusive common traits.

(15) Inagaki, S.; Fujimoto, H.; Fukui, K. *Chem. Lett.* **1976**, 749−752.

**SCHEME 6. *Z*- and *E*-Configured Enecarbamates 1k for the Attack of Singlet Oxygen from below the Plane of the Paper**

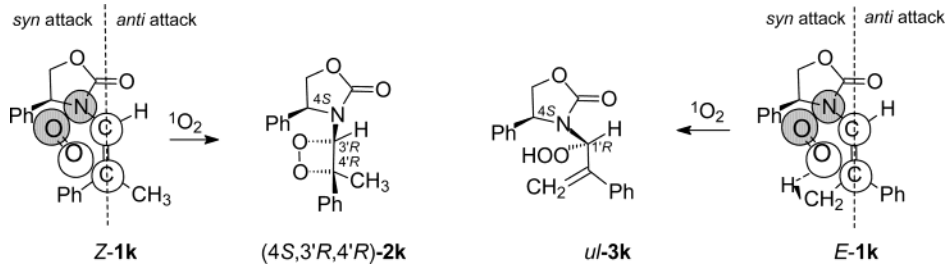


**Mode Selectivity in the Photooxygenation.** From the results in Table 2 it is clear that the mode selectivity of the substrates may be divided into two groups: The *E* isomers react preferentially according to ene mode, whereas for the *Z* isomers the [2+2] cycloaddition is favored. This diastereomer-dependent dichotomy may be understood in terms of the orbital-directing effect of the vinylic nitrogen functionality. The orbital interaction between the HOMO (Figure 5, for (*Z*,4*S*)-**1k**) of the enecarbamate and the LUMO of the incoming singlet oxygen directs the attack onto the side that bears the nitrogen atom (Scheme 6). Since for the enecarbamates ***Z*-1** no allylic hydrogen atom is present on this side of the double bond, [2+2] cycloaddition takes place preferably (entries 15 and 20−23). The [4+2] cycloaddition may compete when the double bond and the phenyl substituent are essentially coplanar, as is presumably the case for substrate ***Z*-1*l*** (Table 2, entry 23).

In contrast to *Z*-**1**, in the enecarbamates ***E*-1** the directing nitrogen atom of the enamine functionality and the methyl group are located on the same side of the double bond. Thus, the incoming singlet oxygen abstracts an allylic hydrogen atom from the methyl group and a high mode selectivity in favor of the ene reaction is expressed (entries 14 and 16−19). In the case of the substrates **1a**−**g**, not even traces of ene reaction are observed (Table 2, entries 1−13). The reason for this is that not only does the vinylic nitrogen atom favor [2+2] cycloaddition, but also 1,2-allylic strain disfavors the competing ene reaction. As the first conformer of the enecarbamates **1a**−**g** in Figure 6 conveys, the allylic hydrogen atom to be abstracted cannot assume a coplanar alignment with the $\pi$ orbital of the CC double bond because of steric repulsion between the methyl group at the chirality center and the vinylic phenyl substituent (Figure 6).

**Diastereoselectivity in the [2+2] Cycloaddition of Singlet Oxygen.** The high diastereoselectivity in the [2+2] cycloaddition of singlet oxygen is demonstrated by all chiral substrates **1b**−**g** (Table 2, entries 2−13). Thus,

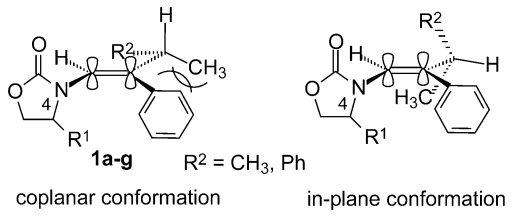


**FIGURE 6.** Sterically hindered coplanar and preferred in-plane conformations of the abstractable allylic hydrogen atom in the enecarbamates **1a**−**g**.

**SCHEME 7. Preferred $\pi$-Facial Attack of Singlet Oxygen, Controlled by Steric Shielding of the $R^1$ Substituent in the Enecarbamate 1**

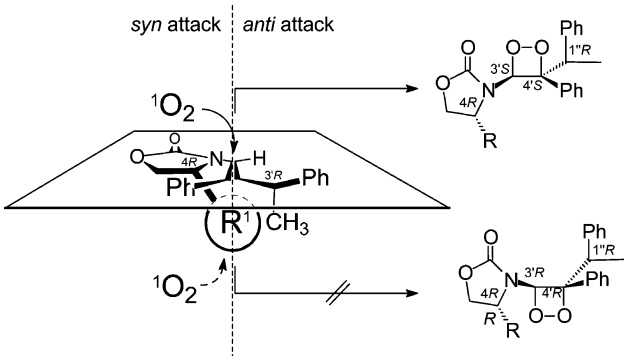


already a methyl group in the oxazolidinone ring suffices to obtain perfect $\pi$-facial control (Table 2, entries 2 and 3), a fact that illustrates the efficacious steric shielding inherent in these enecarbamates. This is accentuated by the finding that no diastereoselectivity is observed in the absence of chirality in the oxazolidinone ($R^1$ = H, entry 1).

From the results in Table 2 it becomes evident that the *R*-configured $R^1$ substituents induce two new *S*-configured stereogenic centers (entries 2−5, 7−8, and 13), as shown in Scheme 7. In contrast, the *S*-configured $R^1$ substituents afford the inverse diastereoselectivity (entries 6 and 9−12). Furthermore, the configuration at the C3′ position of the enecarbamate (Scheme 7) does not influence the diastereoselectivity, as is demonstrated by the fact that the attack of singlet oxygen takes place from the same $\pi$ face, irrespective of whether the 3′*R*- or 3′*S*-configured enecarbamate (*Z*,4*R*,3′*R*)-**1c** or (*Z*,4*R*,3′*S*)-**1c** (entries 4 and 5, Table 2) is employed. Furthermore, the complete diastereoselectivity observed in the case of the enecarbamate (*Z*,4*R*)-**1g** ($R^2$ = $^i$Pr, entry 13), in which the phenylethyl substituent is replaced by an isopropyl group, confirms that only the stereogenic center on the oxazolidinone dictates the $\pi$-facial selectivity. This effect is in part due to the steering nature of the vinylic nitrogen functionality, which promotes syn attack of singlet oxygen (Scheme 7).

Furthermore, the diastereoselectivity of the photooxygenation of enecarbamate (*Z*,4*R*,3′*R*)-**1c** is independent of the solvent polarity (entries 7 and 8, Table 2), which suggests that the carbonyl group plays no significant role in the stereochemical outcome of the [2+2] cycloaddition. This is in good agreement with the X-ray structure of (*Z*,4*R*,3′*S*)-**1c** (Figure 1), which shows that the carbonyl group points away from the double bond functionality and

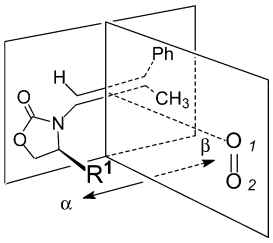


**FIGURE 7.** Fukui's polarity model of singlet oxygen applied to the photooxygenation of the enecarbamate substrate.

is too remote to interact sterically and/or electronically with the attacking $^1O_2$. Thus, the high diastereoselectivity in the dioxetane formation from the ***Z*-1i−*l*** enecarbamates (Table 2, entries 20−23) may be explained in terms of the synergistic interplay between the directing vinylic nitrogen effect and the effective shielding of one of the $\pi$ faces of the CC double bond by the $R^1$ substituent (Scheme 7). Unfortunately, the diastereoselectivity of the [2+2] cycloaddition for the enecarbamates ***E*-1i−*l*** could not be assessed (Table 2, entries 16−19), because these dioxetanes decompose during the photooxygenation.

**Diastereoselectivity in the Ene Reaction of Singlet Oxygen.** The diastereoselectivity of the ene reaction, like the mode selectivity, depends strongly on the double bond configuration of the enecarbamate (Figure 3). In the case of the ***Z*-1i−*l*** derivatives (entries 20−23, Table 2), relatively little (13−25%) ene product is formed and the diastereoselectivity depends strongly on the steric hindrance of the $R^1$ substituent, which follows the order Me $^i$Pr < Ph ≪ $^t$Bu. In fact, to obtain the ene product, an anti attack of singlet oxygen must occur with respect to the $R^1$(Ph) substituent (Scheme 6), because the methyl group with the abstractable hydrogen atoms is on the opposite side and less likely accessible. In the case of the methyl and isopropyl $R^1$ substituents (Table 2, entries 20 and 21), the steric shielding is not sufficiently effective to obtain appreciable diastereofacial differentiation in the anti attack (entries 20 and 21, Table 2). On the contrary, the phenyl and *tert*-butyl $R^1$ substituents (entries 22 and 23) are sufficiently spacious to cover up one $\pi$ face of the double bond and block hydrogen abstraction from the anti direction.

In the case of the ***E*-1** substrates, the oxazolidinone ring is on the same side of the double bond as the methyl group (Scheme 6). Thus, through the steering effect of the vinylic nitrogen, the singlet oxygen enters the double bond from the side of the oxazolidinone ring (syn attack) and encounters more severe steric interactions with the $R^1$ substituent. Accordingly, the diastereoselectivity in the ene reaction of the ***E*-1** substrates is generally higher (entries 16−19, Table 2) than that for the corresponding *Z* isomer (entries 20−23) and already a methyl substituent gives about the same diastereoselectivity (88:12) as a *tert*-butyl substituent (91:9).

The generally lower diastereoselectivity of the ene reaction with respect to the [2+2] cycloaddition depends on the distinct steric interactions between the incoming singlet oxygen and the $R^1$ substituent for these two reaction modes. According to Fukui's theoretical analysis,[15] the alignment of the approaching O-1 atom (Figure 7) determines whether the α or $\beta$ region of the double bond will be attacked, which in turn depends on the polarization of the CC double bond. Electron-rich substituents in the α region increase the electron density in the $\beta$ region through conjugation (+M effect) and the attack will be preferred there. This implies an asymmetric perepoxy-like structure for the transition state, with the O-1 atom closer to the double bond in the $\beta$ region. For the ene reaction, the steric interaction with the substituent $R^1$ is less severe, because the terminal O-2 atom is closer to the methyl group for the hydrogen abstraction, whereas in the [2+2] cycloaddition, the terminal O-2 atom must come into the α region to cyclize the dioxetane ring and the interaction with $R^1$ is much more intensive.

**Diastereoselectivity in the DMD and mCPBA Epoxidations.** The epoxidation of the enecarbamate **1j−*l*** showed also a high degree of diastereoselectivity (Table 3), although not as high as for the photooxygenations (Table 2). The diastereoselectivity of the epoxidation is again controlled by the $R^1$ substituent of the oxazolidinone ring, since the epoxidation of the parent achiral enecarbamate **1h** ($R^1$ = H) is unselective (Table 3, entries 1 and 2). Moreover, the configuration of stereogenic center in the oxazolidinone ring determines the absolute configuration of the epoxide product, that is, the *R* configuration in the enecarbamate *Z*-**1j** (entries 3 and 4, Table 3) leads mainly to the (4*R*,2′*S*,3′*S*)-**4j** product, whereas the *S* configuration in the substrates *Z*-**1k** (entries 5 and 6) and *Z*-***1l*** (entries 7 und 8) affords mainly the corresponding 2′*R*,3′*R* epoxides.

To account for the fact that the size of the $R^1$ substituent dictates the extent of the diastereoselectivity of the epoxidation, we propose the mechanism in Figure 8 for the oxygen transfer, in which for convenience of comparison the attacks from above and below for both the *E* and the *Z* diastereomers are given. When X = H, the steric hindrance for the 1′*Re*,2′*Re* attack is more or less the same as that for the 1′*Si*,2′*Si* attack, since a favorable conformation may be selected in which the methyl groups are out of the way of the incoming oxidant. When, however, $R^1$ is a *tert*-butyl group (X = $CH_3$ in Figure 9) as in the enecarbamate Z-***1l*** (entries 7 and 8, Table 3), the 1′*Re*,2′Re attack is severely obstructed and the highest 1′*Si*,2′*Si* diastereoselectivity (dr = 7:93) is obtained; the (**2′*R***,3′*R*)-***4l*** epoxide is formed almost exclusively for both oxidants DMD and *m*CPBA.

The preferably attacked $\pi$ face remains the same for the *Z*- or *E*-configured enecarbamates, i.e., the 1′*Si*,2′*Si* face for the Z and the 1′*Si*,2′*Re* face for the *E* isomer in Figure 8; however, the extent of the diastereofacial differentiation depends decisively on the double bond configuration, as manifested by the fact that the epoxidation of the *Z* isomers is always more selective than that of the *E* isomers. This difference is due to the conformational effects in the *Z* and *E* isomers, which express the shielding efficacy of the double bond in the enecarbamate. As may be seen from the lowest energy conformations of the ***E*-1*l*** and ***Z*-1*l*** isomers calculated by the DFT method (see the Supporting Information), the shielding of the upper face of the double bond, i.e., 1′*Re*,2′*Re* for *Z*-***1l*** and the 1′*Re*,2′*Si* for *E*-***1l*** (Figure 8), by the $^t$Bu group is more effective in the case of the *Z* than the *E* diastereomer. Expectedly, the 1′*Si*,2′*Si* attack should be facilitated for the *Z* case, as is documented by the higher dr values for the *Z*-***1l*** substrate (Table 3, entries 7 and 8) versus those

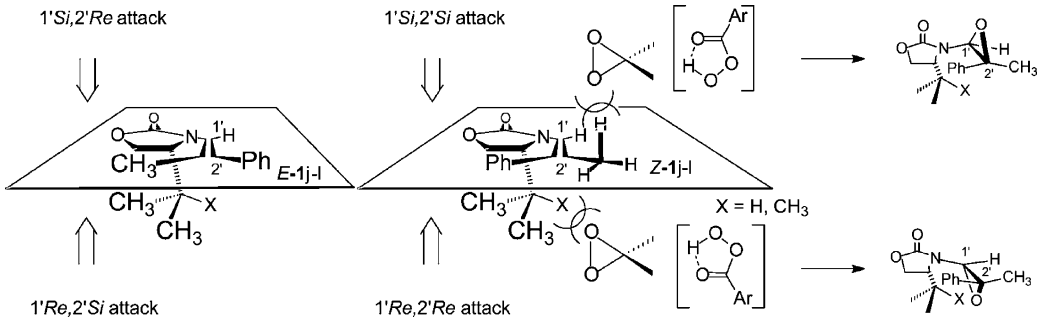


**FIGURE 8.** Preferred $\pi$-facial attack of the DMD epoxidation as a function of the size of the X substituent in the enecarbamates *E*-**1j**,***l*** and *Z*-**1j**,***l*** (X = H, $CH_3$).

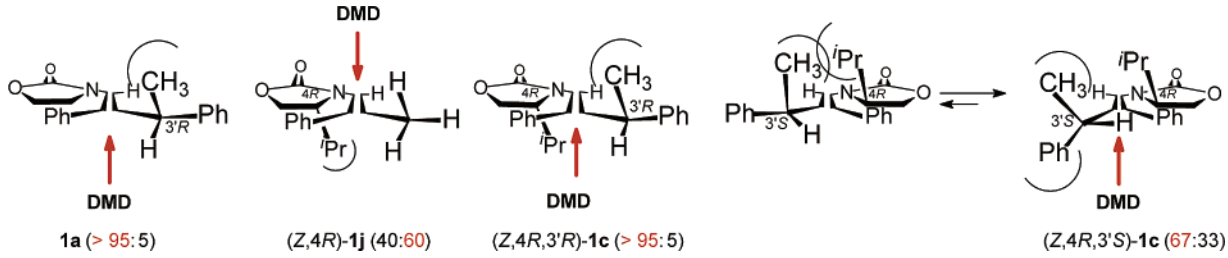


**FIGURE 9.** Preferred configurations for the *match*/*mismatch* effect in the *Z*,4*R*,3′*R* and *Z*,4*R*,3′*S* diastereomers of the enecarbamate **1c** versus the *Z*,3′*R* enantiomer of **1a** and the *Z*,4*R* enantiomer of **1j**.

for *E*-**1*l*** (entries 15 and 16). Thus, only the large steric demand of a *tert*-butyl group suffices to cover up the double bond sufficiently in the *E*-configured enecarbamate **1*l*** to induce an appreciable diastereoselectivity.

**The *Match*/*Mismatch* Effect in the Epoxidation.** The *match*/*mismatch* effect in the epoxidation is documented for the set of enecarbamates **1a** (only the phenylethyl stereogenic center), the diastereomeric pair (*Z*,4*R*,3′*R*)-**1c** and (*Z*,4*R*,3′*S*)-**1c** (both stereogenic centers), and (*Z*,4*R*)-**1j** (only the oxazolidinone stereogenic center), whose stereoprojections are given in Figure 9. In the enecarbamate **1a**, the phenylethyl substituent fully controls the attack of the DMD on the double bond (Figure 9), since complete diastereoselectivity is observed (Table 3, entry 17). Within the phenylethyl substituent, the phenyl group is sterically more demanding and, thus, points away from the remaining substrate (Figure 9). Since the hydrogen atom at the chirality center is sterically less demanding than the methyl group, it is oriented toward the double bond, while the methyl group shields the $\pi$ face above the double bond. Consequently, the DMD attack takes place preferably from the bottom $\pi$ face and leads to the (2′*R**,3′*R**,1″*R**)-**4a** epoxide.

In the epoxidation of the diastereomeric enecarbamates (*Z*,4*R*,3′*R*)-**1c** and (*Z*,4*R*,3′*S*)-**1c**, the complete diastereoselectivity for (*Z*,4*R*,3′*R*)-**1c** indicates that this constitutes the *matched* case (Table 3, entry 18), whereas the low diastereoselectivity of 67:33 (entry 19) for the epoxidation of (*Z*,4*R*,3′*S*)-**1c** suggests that this is the *mismatched* situation. From the steric interactions displayed in Figure 9, it becomes evident that the phenyl group of the phenylethyl substituent in (*Z*,4*R*,3′*R*)-**1c** points away from the rest of the substrate to minimize 1,2-allylic strain. In this preferred conformation, the methyl group of the phenylethyl substituent hinders the attack from the upper side of the double bond and overcompensates for the influence of the isopropyl group on the oxazolidinone ring. This is substantiated by the fact that little control in the diastereoselectivity is observed for the epoxidation of the enecarbamate (*Z*,4*R*)-**1j**, which possesses only chirality in the oxazolidinone ring (Figure 9).

In the (*Z*,4*R*,3′*S*)-**1c** diastereomer, the $R^1$ substituent of the oxazolidinone sterically interacts with the phenylethyl substituent on the CC double bond (Figure 9) in competition with 1,2-allylic strain. Consequently, the steric repulsion between the methyl and the isopropyl groups populates a minimum-energy conformation in which the methyl substituent obstructs the attack of the oxidant DMD on the upper $\pi$ face, whereas the phenyl group of the phenylethyl substituent shields the lower $\pi$ face. Thus, the (*Z*,4*R*,3′*S*)-**1c** diastereomer constitutes the *mismatch* case, for which a much lower (67:33) diastereoselectivity (entry 17) is observed.

That in the epoxidation the phenylethyl substituent controls the diastereoselectivity better than the oxazolidinone auxiliary contrasts the results seen in the photooxygenation, for which the reverse situation applies. This divergence may be explained in terms of the following two factors: On one hand, DMD is larger than singlet oxygen and, thus, the steric interactions of the phenylethyl substituent at the double bond are more intensive; on the other hand, the steering effect of the vinylic nitrogen atom in singlet-oxygen attack accentuates the steric interactions with the $R^1$ substituent of the oxazolidinone auxiliary.

**Synthetic Application.** The highly diastereoselective photooxygenation of the enecarbamate **1** offers the opportunity to exploit these advantageous substrates for the synthesis of valuable, optically active building blocks.[16] For example, the reduction of the dioxetanes **2** to optically active diols constitutes such a utilization of this unprec-

(16) Kolb, H. C.; VanNieuwenhze, M. S.; Sharpless, B. K. *Chem. Rev.* **1994**, *94*, 2483−2547.

**SCHEME 8. Synthesis of the Optically Active Enecarbamates 1, Their Stereoselective Oxidation to the Respective Dioxetanes 2 and Epoxides 4, Their Transformation to the Enantiomerically Enriched Diols 8−10, and the Recyclization of the Chiral Oxazolidinone Auxiliary**

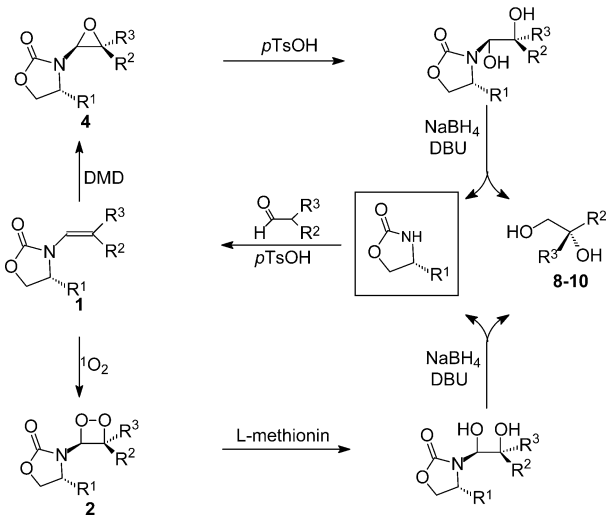


edented oxidation chemistry (Scheme 8). The chiral oxazolidinone auxiliary may be recovered after the reductive cleavage and recycled. Clearly, this represents an attractive feature of our new asymmetric oxidation methodology.

Similarly, the epoxidation by DMD and *m*CPBA (Scheme 8) entails an alternative highly diastereoselective route to the same enantiomerically enriched oxyfunctionalized products. All the advantages of the substrate-controlled selectivities for the photooxygenation are inherent in the epoxidation process, which should establish itself as an attractive tool for the synthesis of asymmetric oxyfunctionalized compounds.

## Mechanistic Synopsis

The present mechanistic work on the diastereoselectivity and mode selectivity in the photooxygenation ($^1O_2$) and epoxidation (DMD, *m*CPBA) of the enecarbamates **1** has revealed that the characteristic structural and electronic features of these substrates are decisively responsible in steering the attack of the oxidant. The structural characteristics encompass the $R^1$ substituent in the oxazolidinone chiral auxiliary, the *E*,*Z* configuration of the double bond, and the stereogenic substituent on that functionality, while the electronic factor relates to the enamine-type double bond. The structural aspects provide the necessary steric interactions toward the incoming oxidant through proper conformational alignment, and the electronic feature is expressed in terms of the stereoelectronic control through the enamine-type nitrogen functionality. The salient consequences of these factors on the selectivities (mode and diastereo) of the photooxygenation ($^1O_2$) and epoxidation (DMD and *m*CPBA) will now be highlighted, first for the stereoelectronic and subsequently for the steric effects.

**The Stereoelectronic Effect of the Vinylic Nitrogen Functionality.** The observed *E*,*Z*-dependent mode selectivity of $^1O_2$ is caused by the favorable HOMO-LUMO interaction with the vinylic-nitrogen functionality, which steers the enophile toward the syn side of the double bond with respect to the oxazolidinone. When this side bears a methyl group, allylic hydrogen abstraction takes place and the ene product is formed; when, however, the phenyl group is located cis to the oxazolidinone substituent, [2+2] cycloaddition occurs. For the latter reaction mode, the synergistic interplay between the vinylic nitrogen functionality and the shielding by the $R^1$ substituent cause the diastereoselectivity in the [2+2] cycloaddition to be essentially perfect (dr > 95:5) already for the relatively small methyl group. The bulky phenylethyl substituent on the CC double bond plays no significant role, because the singlet oxygen attacks the *Z* diastereomer anti to the phenylethyl group due to the steering by the vinylic nitrogen functionality. In contrast, in regard to diastereoselectivity, the vinylic nitrogen functionality is inconsequential for the epoxidation. Although it would be expected that by increasing the size of the oxidant (DMD versus $^1O_2$) the diastereoselectivity should increase, the highest dr value for the epoxidation is at best 93:7 versus >95:5 for the photooxygenation. This is the consequence of the lack of stereoelectronic steering by the vinylic nitrogen functionality for DMD versus $^1O_2$. Contrary to $^1O_2$, DMD attacks anti to the oxazolidinone substituent to avoid the steric hindrance by the $R^1$ substituent.

**The Steric Effects of the $R^1$ Substituent on the Oxazolidinone Auxiliary.** The favored conformation of the enecarbamates **1** in solution positions the $R^1$ substituent of the chiral auxiliary to one $\pi$ face of the double bond, thereby it sterically shields the incoming oxidant ($^1O_2$, DMD, and *m*CPBA) and causes a highly diastereoselective attack from the opposite side. The size of $R^1$ strongly influences the extent of the shielding and thereby the diastereoselectivity of the ene reaction. Although for both the [2+2] cycloaddition and the ene reaction a perepoxy-like transition state is traversed, the allylic hydrogen abstraction in the ene reaction occurs far away from the $R^1$ substituent and the steric interactions are not as effective as in the case of the [2+2] cycloaddition, in which the tailing oxygen atom must come near the $R^1$ substituent to close the dioxetane ring. Thus, the control of the diastereoselectivity in the singlet-oxygen ene reaction is lower than that of the [2+2] cycloaddition. The size of the $R^1$ substituent also influences the diastereoselectivity in the epoxidation reactions, in which a sterically demanding substituent such as the bulky *tert*-butyl group may completely cover one face of the double bond and encumber the attack of the oxidant from that direction.

**The Steric Effects of the Phenylethyl Substituent on the CC Double Bond.** This bulky, chiral phenylethyl substituent as the only stereogenic center in the enecarbamate may control completely the diastereoselectivity of the DMD epoxidation, whereas it exercises no influence in the singlet-oxygen [2+2] cycloaddition and ene reaction. Through the vinylic-nitrogen steering effect, the phenylethyl group is not on the trajectory of the incoming $^1O_2$. DMD is sterically significantly more demanding than $^1O_2$ and encounters severe hindrance by the phenylethyl group such that substantial diastereoselectivity is obtained during the epoxidation.

**The Composite Steric Effects of the $R^1$ and the Phenylethyl Substituents.** The steric interactions between two stereogenic centers, namely the phenylethyl substituent at the CC double bond and the $R^1$ group of the oxazolidinone auxiliary, may influence the diastereoselectivity of the oxidation, a phenomenon known as the "*match*−*mismatch*" effect. For the epoxidation, the $R^1$ group (e.g. isopropyl) alone causes little diastereofacial differentiation, but a high diastereoselectivity is imposed by the phenylethyl group alone; for the photooxygenation, the opposite applies. On one hand, are both stereogenic centers present, when they occupy different half-spaces above and below the CC double bond, they do not sterically interact with one another and the phenylethyl group controls completely the diastereoselectivity. On the other hand, when the two substituents occupy the same half-space, conformational changes are imposed by their mutual steric interactions and the diastereoselective control is severely reduced. These effects play only a role in the epoxidation and none in the photooxygenation because, as already stated, $^1O_2$ is not subject to diastereoselective control by the phenylethyl group.

**The Conformational Effects of the *E*/*Z* Configurations.** For the *Z*-configured enecarbamates the shielding is substantially better than that for the corresponding *E*-configured isomers because of conformational alignment of the double bond substituents, which is reflected in the higher diastereoselectivity of the *Z* versus the *E* isomers with DMD and *m*CPBA, but not for $^1O_2$. For the latter, the stereoelectronic steering by the vinylic nitrogen functionality overcomes the influence of the *E*/*Z* configurations in the case of the ene reaction. For the [2+2] cycloaddition of $^1O_2$, no conclusions may be drawn because the dioxetanes could only be detected for the *Z* diastereomers (diastereoselectivity >95:5).

**Acknowledgment.** This work was generously supported by the Deutsche Forschungsgemeinschaft (Schwerpunktprogramm "Peroxidchemie") and the Fonds der Chemischen Industrie. We thank M. Schwarm (Degussa Hüls AG, Hanau) for a generous gift of the optically active oxazolidinones and alaninol, J. Bialas for the synthesis of DMD, and H. Ihmels for helpful discussion, and K. Wissel for valuable assistance.

**Supporting Information Available:** Experimental details and X-ray crystallographic data for (*Z*,4*S*)-**1k**. This material is available free of charge via the Internet at http://pubs.acs.org.

JO035745C